FRACTURE TOUGHNESS OF BRITTLE MATERIALS DETERMINED WITH CHEVRON NOTCH SPECIMENS

J. L. Shannon, Jr.*, R. T. Bubsey*, D. Munz** and W. S. Pierce*

INTRODUCTION

Increasing world-wide energy consumption has stimulated activity in the fields of coal and oil extraction and in energy conversion and usage systems such as coal gasifiers and high-temperature gas turbine engines. The role of fracture mechanics in these fields has grown, pointing to the specific need for standard test methods for determining the plane strain fracture toughness K_{Ic} of brittle nonmetallic materials, principally rocks and ceramics.

Current fracture tests make use of a variety of specimen types (single edge bend, double torsion, double cantilever bend, and surface flawed specimens) having either blunt notches produced by saw cutting, or cracks produced by wedge loading, indenting, or local thermal shock. Specimens with blunt notches can overestimate K_{Ic}. Precracked specimens are difficult to prepare in a reproducible manner, and the initial crack front often cannot be seen on the fracture surface after testing, making it nearly impossible to measure the initial crack length. These current difficulties can be overcome by using a specimen containing a chevron notch in which a crack originates at the tip of the triangular ligament during loading. Specimens with a chevron notch were first used by Nakajam [1] in work of fracture studies, and later by Tattersall and Tappin [2] for fracture surface energy measurements. More recently, Barker [3] has proposed a chevron-notch specimen for plane strain fracture toughness measurement. The essential features of the chevron-notch specimen are that (1) a sharp natural crack is produced during the early stage of test loading (no precracking is required) and (2) the load passes through a maximum at a constant material-independent crack length-to-width ratio for a specific specimen geometry (no post-testcrack length measurement is required). For materials with flat crack growth resistance curves, the plane strain fracture toughness K_{Ic} is proportional to the maximum test load, and a function of the specimen geometry and elastic compliance.

A development program on three chevron-notch specimens (short bar, short rod, and four-point-bend (see Figure 1))has been underway at the NASA-Lewis Research Center Cleveland, Ohio, U.S.A., for the past three years. Stress intensity factor coefficients have been developed, both analytically and experimentally, and fracture toughness measurements on Si_3N_4 and Al_2O_3 have been made to assess the performance of each specimen type. Due to page limitations in this volume, only the short bar configuration will be treated in this paper. Results for the other two configurations may be found in references [4] through [7] .

STRESS INTENSITY FACTOR

The chevron notch (Figure 1) is characterized by the notch length at the specimen surface, a_1; the notch length to the tip of the chevron, a_o; and the specimen width, W, and thickness, B. The shaded areas in Figure 1 represents cracks of length a. The crack front length b is

$$b = B\frac{a - a_o}{a_1 - a_o} = B\frac{\alpha - \alpha_o}{\alpha_1 - \alpha_o} \qquad (1)$$

where $\alpha = a/w$, $\alpha_o = a_o/w$, and $\alpha_1 = a_1/w$

*NASA-Lewis Research Center, Cleveland, Ohio, 44135, U.S.A.
**Universität Karlsruhe and Kernforschungszentrum Karlsruhe, Karlsruhe, FR Germany

The relation between maximum load P_{max} and fracture toughness K_{Ic}*is obtained by equating the available and the necessary energies for crack propagation. The energy available to extend the crack a small increment Δa is

$$\Delta U = \frac{P^2}{2W} \cdot \frac{dC_{tr}}{d\alpha} \cdot \Delta a \qquad (2)$$

where C_{tr} is the elastic compliance of the chevron-notch specimen; the subscript "tr" denoting the fact that in the chevron-notch specimen, the crack proceeds through the chevron notch such that the two together constitute a discontinuity with a trapezoidal front. The energy necessary to extend the crack by the increment Δa is

$$\Delta \bar{W} = G_{Ic}\, b\, \Delta a = \frac{K_{Ic}^2}{E'} \cdot b \cdot \Delta a \qquad (3)$$

with elastic modulus E' = E for plane stress and E' = E/(1-ν^2) for plane strain.**

During crack extension, $\Delta U = \Delta \bar{W}$, leading to

$$K_{Ic} = P \left[\frac{(dC_{tr}/d\alpha)E'}{2Wb}\right]^{\frac{1}{2}} = \frac{P}{B\sqrt{W}} \left[\frac{1}{2} \frac{dC'_{tr}}{d\alpha} \frac{\alpha_1-\alpha_o}{\alpha-\alpha_o}\right]^{\frac{1}{2}} \qquad (4)$$

where $C'_{tr} = E'BC_{tr}$ is the dimensionless compliance. The term

$$Y^* = \left[\frac{1}{2} \frac{dC'_{tr}}{d\alpha} \frac{\alpha_1-\alpha_o}{\alpha-\alpha_o}\right]^{\frac{1}{2}} \qquad (5)$$

is the dimensionless stress intensity factor coefficient. Maximum load occurs at the minimum of the term in brackets, and is designated Y^*_m.

*The authors recognize that the designation K_{Ic} is customarily reserved for that value of plane strain fracture toughness determined in strict accordance with the ANSI/ASTM E-399 Standard Test Method for Plane - Strain Fracture Toughness of Metallic Materials. However, for materials with flat crack growth resistance curves (i.e., extremely brittle materials), we believe the chevron-notch specimen would yield a plane strain fracture toughness value fully equivalent to K_{Ic} of the E-399 test, and without the encumbrances of post-test crack length measurement and secant-line construction on the test record; therefore, the toughness values obtained in this investigation are designated K_{Ic}.

**There is some uncertainty about the usage of the plane strain or plane stress relation when stress intensity factors are derived from compliance measurements [8]. Whereas there is plane strain in the immediate vicinity of the notch at mid thickness, the bulk of the specimen is nearer the plane stress state. Therefore, Brown and Srawley [9] have proposed to omit the (1 -ν^2) term for E'.

There are no available analytical solutions for the chevron-notch short bar specimen stress intensity factor coefficient. However, as a first approximation it can be assumed that $dC'_{tr}/d\alpha$ for the chevron notch with a crack is identical to that $dC/d\alpha$ for a straight-through crack. This approximation is referred to as the "straight-through crack assumption", STCA. Using the relation for a straight-through crack

$$\frac{dC}{d\alpha} = 2Y^2 \qquad (6)$$

where

$$Y = \frac{KB\sqrt{W}}{P},$$

Eqs. (4) and (5) can be rewritten

$$K_{Ic} = \frac{P}{B\sqrt{W}} Y \left[\frac{\alpha_1-\alpha_o}{\alpha-\alpha_o}\right]^{\frac{1}{2}} \qquad (7)$$

and

$$Y^* = Y \left[\frac{\alpha_1-\alpha_o}{\alpha-\alpha_o}\right]^{\frac{1}{2}} \qquad (8)$$

where Y* is the chevron-notch and Y the straight-through crack specimen coefficients.

The dimensionless stress intensity factor coefficient for the short bar specimen with a straight-through crack is (10):

$$Y = \frac{\alpha}{(1-\alpha)^{3/2}} \ln\left(\exp\left[\frac{2.702}{\alpha} + 1.628\right] + \exp\left\{\left[12\frac{W^3(1-\alpha)^3}{H^3}\right]^{\frac{1}{2}}\left[1+\frac{0.679}{\alpha(W/H)}\right]\right\}\right) \qquad (9)$$

To check the validity of the straight-through crack assumption, a series of short bar experimental compliance measurements were made [10]. The compliance specimens were machined in the L-T crack plane orientation from 7075-T651 aluminum plate to the dimensions shown in Figure 2a for W/H ratios of 3 and 4. A 17.8 mm slot was machined into the front face to accommodate loading knife edges (Figure 2b). The displacements measurements were made with a modified ASTM E-399 clip-in gage as shown in Figure 2c. Hardened steel cones were fastened to the inner surfaces of the displacement gage arms and set into small indentations in the top and bottom of the specimens [6]. A 0.6 mm slot was extended incrementally to simulate an advancing crack in the specimen.

The compliance results for specimen proportioned W/H = 4 are presented as functions of the notch parameters α_o in Figures 3 and α_1 in Figure 4. The results for specimen proportioned W/H = 3 were, of course, quite similar. The compliance curves were differentiated to obtain $dC'_{tr}/d\alpha$ for substitution into Eq. (5)

for the stress intensity factor coefficient Y*. Y*'s obtained in this way from Figure 3 are compared in Figure 5 with Y*'s obtained analytically using the STCA relation of Eqs. (8) and (9).

In the region of the curve minima, designated Y^*_m and indicated by arrows to the curves, the experimental and analytical results agree extraordinarily well: less than 4 percent difference for the greatest initial crack length (α_o=0.495), and less than 1 percent difference for the two shorter initial crack lengths. As expected, the minima decrease and broaden with decreasing α_o. Location of the minima at α_m corresponding to maximum load (and Y^*_m) varies in such a way that the quantity $(\alpha_m-\alpha_o)$, which is the relative crack extension up to maximum load, passes through a maximum as shown in Figure 6.

Experimental results showing the influence of α_1 on Y* are shown in Figure 7. Decreasing α_1 lowers the curves and, at $\alpha = \alpha_1$, the chevron-notch specimen curves join the curve for a straight-through crack specimen. According to the straight-through crack assumption, the location of the curve minima should not vary; e.i. the relative crack length at maximum load α_m should be independent of α_1 (shown by differentiating Eq. (8) with respect to α for $\alpha = \alpha_m$). Experimentally, however, α_m will vary with α_1, and this too is predictable from the differentiation of Eq. (8) . This dependence of α_m on α_1 produces a continuous rise in the amount of relative crack extension up to maximum load $(\alpha_m-\alpha_o)$ as a function of α_1 as shown in Figure 8.

The minimum values Y^*_m of Y* are used in conjunction with P_{max} to compute K_{Ic}. Since no practical difference was observed between the experimental and analytical Y^*_m values, and for the sake of computational simplicity, the STCA values were used for all K_{Ic} calculations in the toughness measurements portion of this study. Under the STCA, K_{Ic} for the short bar specimen may be expressed:

$$K_{Ic} = \frac{P}{B\sqrt{W}} Y^* \qquad (10)$$

Substituting P_{max} for P and Y^*_m for Y*, K_{Ic} is obtained from maximum load with no need for crack length measurement. For specimens with $\alpha_1 = 1$, and in the range $3 \leq W/H \leq 4$ and $0.2 \leq \alpha_o \leq 0.5$, Y^*_m may be expressed:

$$Y^*_m = \left(4.08 + 3.95\left(\frac{W}{H}\right) + 0.50\left(\frac{W}{H}\right)^2 + \left[-23.15 + 1.15\left(\frac{W}{H}\right) + 1.30\left(\frac{W}{H}\right)^2\right]\alpha_o + \left[172.5 - 43.5\left(\frac{W}{H}\right) + 3.0\left(\frac{W}{H}\right)^2\right]\alpha_o^2\right) \qquad (11)$$

This equation is in agreement with the analytical Y^*_m from Eq. (8) within $\pm$ 0.3%. For $\alpha_1 < 1$, Eq.(11) must be multiplied by $\left[(\alpha_1 - \alpha_o)/(1-\alpha_o)\right]^{\frac{1}{2}}$

FRACTURE TOUGHNESS MEASUREMENTS

Two materials were investigated: Norton Company NC-132 hot pressed silicon nitride (Si_3N_4) and 3M Company Alsimag-614 sintered aluminum oxide (Al_2O_3). The Si_3N_4 was acquired as 150 mm x 150 mm x 10 mm thick plate; the Al_2O_3 as bars 12.7 mm x 12.7 mm x 29.2 mm and 25.4 mm x 25.4 mm x 54.6 mm. Short bar specimens were machined to the dimensions shown in Figure 9. Chevron notches were produced by diamond-impregnated wire sawing or by diamond wheel slotting. Details regarding specimen preparation and test procedure have been given in reference [11].

RESULTS

The plane strain fracture toughness of Si_3N_4 determined with short bar specimens of $\alpha_1 = 1.0$ and $0.17 \leq \alpha_o \leq 0.48$ is plotted in Figure 10. A value of K_{Ic} equal to 4.64 ± 0.11 MNm$^{-3/2}$ appears well established and independent of the dimension α_o. The limited amount of data shown in Figure 11 for specimens with $\alpha_o = 0.20$ and $0.50 \leq \alpha_1 \leq 0.99$ suggests independence of K_{Ic} on α_1 as well, and substantiates the mean K_{Ic} value obtained from the data of Figure 10.

The aluminum oxide chevron-notch short bar specimen geometries varied in α_o, α_1, W/H and absolute size (see Figure 9). Plane strain fracture toughness results are shown in Figures 12 and 13. For chevron notches with $\alpha_1 = 1$, there is a small downward trend in K_{Ic} with increasing initial relative crack length α_o (Figure 12). Over the range investigated, this effect is less than 4 percent. A more interesting feature is the strong dependence of K_{Ic} on specimen thickness and width-to-half height ratio. Comparing mean values of K_{Ic}, the thickness effect appears about double that of the W/H ratio. The results for W/H = 4 exceed those for W/H = 3 by 6 percent for B = 25.4 mm and by 10 percent for B = 12.7 mm. The results for B = 25.4 mm exceed those for B = 12.7 mm by 15 percent for W/H = 4 and by 18 percent for W/H = 3.

The largest effect was produced by variation in the relative length of the chevron notch at the specimen surface, α_1 (Figure 13). K_{Ic} drops nearly 25 percent with decreasing α_1 in the range investigated.

PRACTICAL SIGNIFICANCE OF RESULTS

Implicit in the STCA, and underlying the theoretical base for the chevron notch specimen, is the presumption of a flat crack growth resistance curve for the material tested. When this condition is not met, the chevron-notch specimen will yield K_{Ic} values which vary with specimen geometry and size, and therefore is of questionable usefulness in its present state of development. It would appear that the Si_3N_4 tested in this program does satisfy the requirement of a flat crack growth resistance curve and therefore demonstrates the usefulness of the chevron-notch short bar specimen for plane strain fracture toughness evaluation of this material.

In contrast, the Al_2O_3 material appears to have a rising crack growth resistance curve, as evidenced by the size and geometry dependence of its measured K_{Ic}. Since K_{Ic} is calculated from maximum load, its value will depend on the amount of crack extension up to maximum load, and this will vary with chevron notch geometry (see Figures 6 and 8), specimen size, and specimen proportions, W/H. The effect is to vary the point on the rising crack growth resistance curve at which maximum load occurs. Dependence of the notch parameters α_o and α_1 on the amount of crack growth up to maximum load for the two series of Al_2O_3 specimens in Figures 12 and 13, is shown in corresponding Figures 6 and 8. The results of Figure 12 wherein α_o is the controlling chevron notch parameter are plotted in Figure 14 in terms of the crack extension up to maximum load, and provide in effect a gradually rising crack growth resistance curve. A similar exercise involving the data of Figure 13 (α_1 variable) results in the plot of Figure 15. Surprisingly, the curve of Figure 15, reflecting change in α_1, is much steeper than that of Figure 14 for change in α_o. At this juncture, the authors can offer no explanation for this difference, but clearly the basic effect is due to a rising crack growth resistance curve for the Al_2O_3 material tested.

The range of α_o's investigated was for each specimen size and proportions tested, in the segment of negative slope of the $(\alpha_m - \alpha_o)$ vs α_o curves of Figure 6. It would appear that the slight downward trend of K_{Ic} with increasing

α_o in Figure 12 is due to this effect, although it is surprisingly small compared to the α_1 effect in Figure 13 which is due to no greater trend in $(\alpha_m - \alpha_o)$ vs α_1 in Figure 8.

The authors feel the results of this investigation are precautionary in the use of the chevron notch specimen for materials with rising crack growth resistance curves. Tests of any material for its plane strain fracture toughness cannot be considered conclusive unless specimens of more than one geometry and/or size give the same result.

It would appear also from the results that there is a preferred chevron geometry; namely, $\alpha_o = 0.2$ and $\alpha_1 = 1.0$. These correspond to the maximum amount of crack extension up to maximum load, and therefore should provide the greatest stability of the crack front at the measurement point. This would also provide for the greatest sensitivity to non-flat crack growth resistance curves, and be most selective in applicability of the test, which at this time must be restricted to flat crack growth resistance-type materials.

REFERENCES

1. J. Nakayama, "Direct Measurement of Fracture Energies of Brittle Heterogeneous Materials", J. Am. Ceram. Soc., 48:11 (1965), pp.583-587.

2. H. G. Tattersall and G. Tappin, "The Work of Fracture and Its Measurement in Metals, Ceramics and other Materials", J. Mater. Sci., 1:3 (1966), pp.296-301.

3. L. M. Barker, "A Simplified Method for Measuring Plane Strain Fracture Toughness", Eng. Fracture Mech., 9:2 (1977) pp. 361-369.

4. D. Munz, R. T. Bubsey, and J. L. Shannon, Jr., "Fracture Toughness Determination of Al_2O_3 Using Four-Point-Bend Specimens with Straight-Through and Chevron Notches", J. Am. Ceram. Soc., 63:5-6 (1980), pp. 300-305.

5. D. Munz, J. L. Shannon, Jr. and R. T. Bubsey, "Fracture Toughness Calculation from Maximum Load in Four Point Bend Tests of Chevron Notch Specimens", to be published in Int. J. Fracture.

6. R. T. Bubsey, D. Munz, W. S. Pierce, and J. L. Shannon, Jr., "Compliance Calibration of the Short Rod Chevron-Notch Specimen for Fracture Toughness Testing of Brittle Materials", to be published in Int. J. Fracture.

7. Paper on plane strain fracture toughness determinations on Al_2O_3 using the short rod chevron-notch specimen in preparation.

8. R. T. Bubsey, D. M. Fisher, M. H. Jones and J. E. Srawley, "Compliance Measurements", Experimental Techniques in Fracture Mechanics, Soc. for Experi. Stress Anal. Monograph 1, A. S. Kobayashi, ed., Iowa State Univ. Press and Soc. for Experimental Stress Analysis, Cambridge (1976), pp. 76-95.

9. W. F. Brown, Jr. and J. E. Srawley, Plane Strain Crack Toughness Testing of High Strength Metallic Materials, ASTM STP 410, Am. Soc. for Testing & Materials, Philadelphia (1966).

10. D. Munz, R. T. Bubsey, and J. E. Srawley, "Compliance and Stress Intensity Coefficients for Short Bar Specimens with Chevron Notches", Int. J. Fracture 16:4 (1980), pp. 359-374.

11. D. Munz, R. T. Bubsey, and J. L. Shannon, Jr., "Performance of Chevron-Notch Short Bar Specimen in Determining the Fracture Toughness of Silicon Nitride and Aluminum Oxide", J. Test. Eval., 8:3 (1980), pp. 103-107.

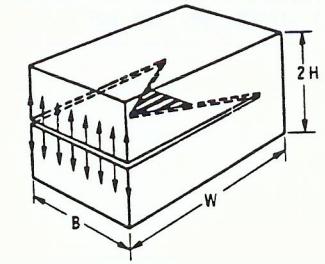

SHORT BAR

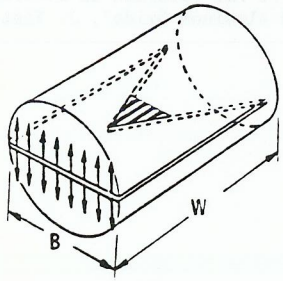

SHORT ROD

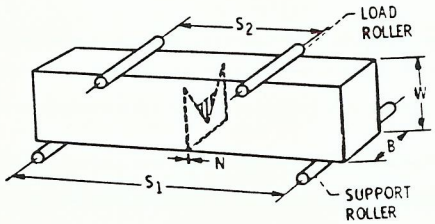

FOUR-POINT BEND

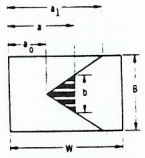

CRACK PLANE SECTION

Figure 1. - Chevron-notch specimens.

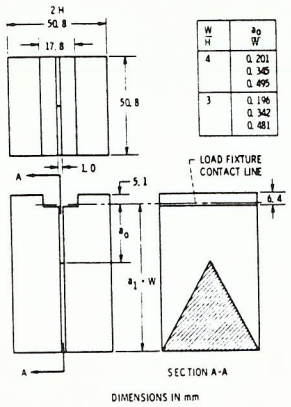

Figure 2a. - Short bar chevron-notch compliance specimen.

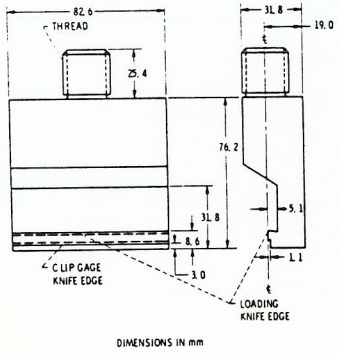

Figure 2b. - Loading fixture.

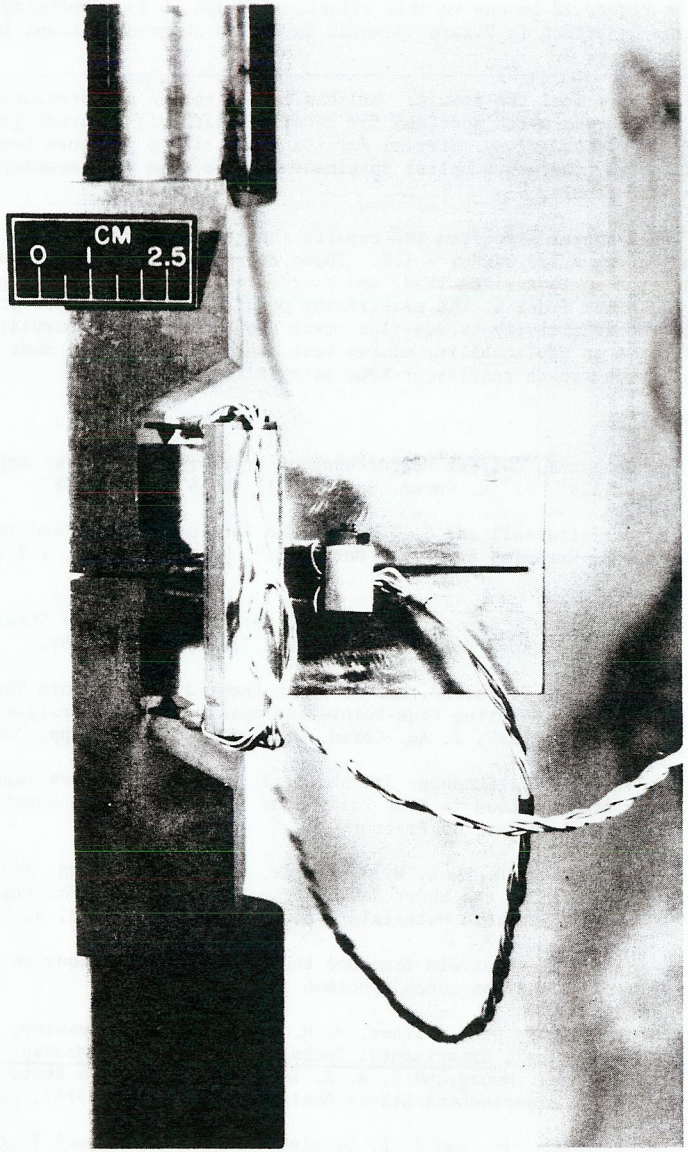

Figure 2c. - Crack mouth opening displacement gage fastened to short bar chevron-notch compliance specimen mounted in loading fixture.

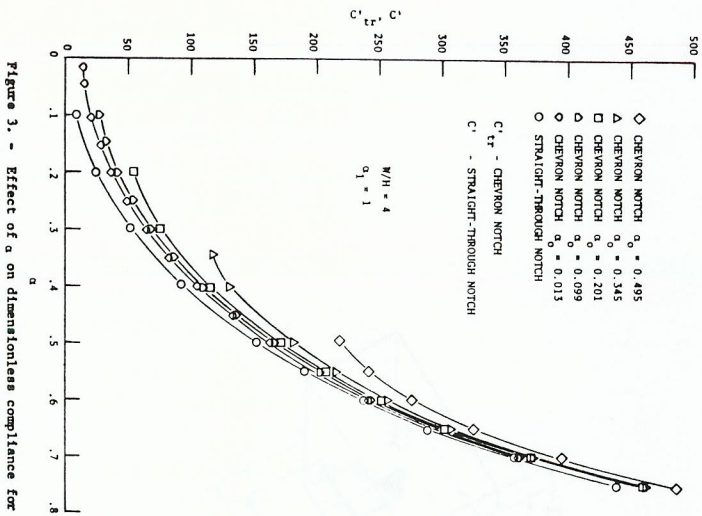

Figure 3. - Effect of α on dimensionless compliance for short bar specimens of W/H = 4 proportions with either a straight-through notch or chevron notches of $\alpha_1 = 1$ and various α_o.

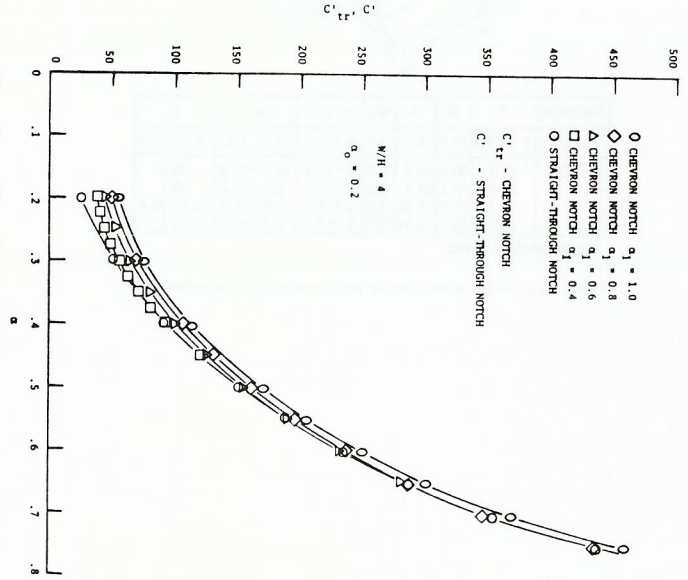

Figure 4. - Effect of α on dimensionless compliance for short bar specimens of W/H = 4 proportions with either a straight-through notch or chevron notches of $\alpha_o = 0.2$ and various α_1.

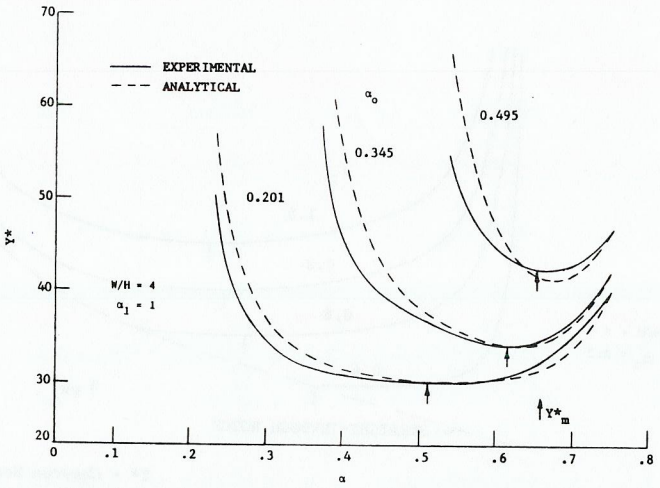

Figure 5. - Stress intensity factor coefficient Y* determined experimentally and analytically for short bar chevron-notch specimens of W/H = 4, $\alpha_1 = 1$, and various α_o.

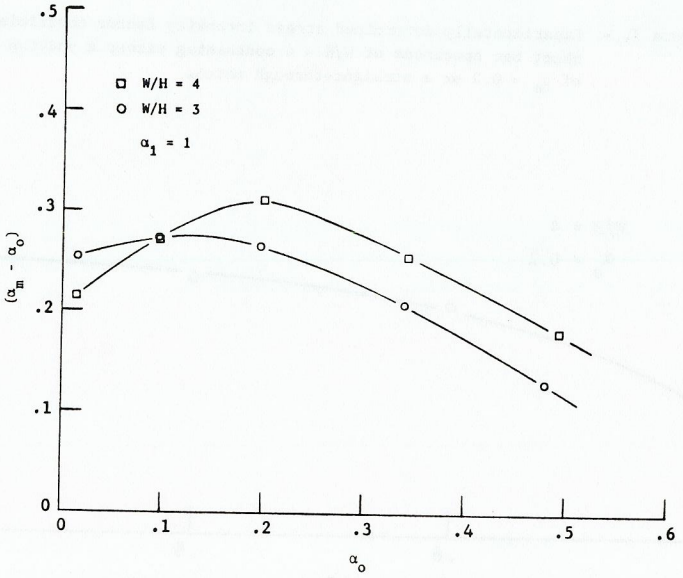

Figure 6. - Relative crack extension $(\alpha_m - \alpha_o)$ at the minimum value of Y* as a function of α_o for short bar chevron-notch specimens of W/H = 3 and 4 and $\alpha_1 = 1$.

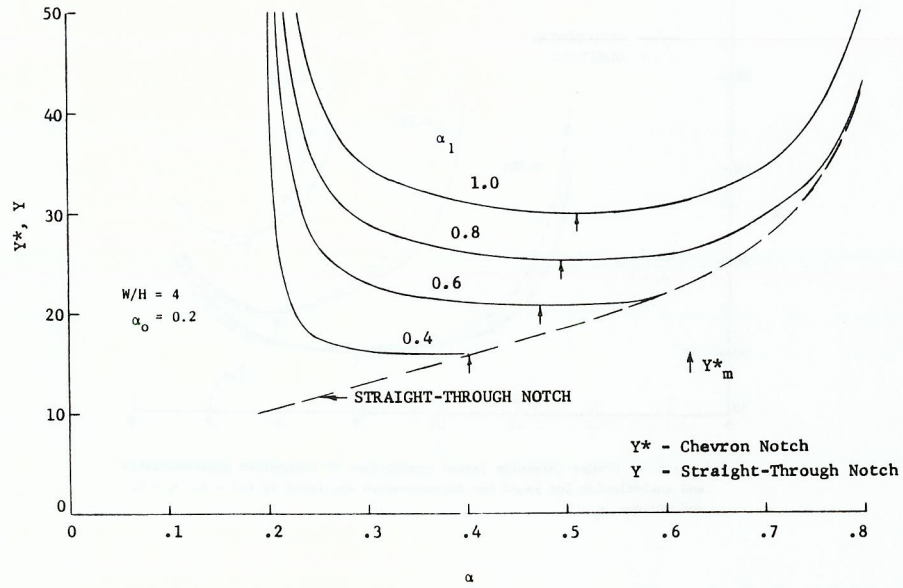

Figure 7. - Experimentally determined stress intensity factor coefficient for short bar specimens of W/H = 4 containing either a chevron notch of α_o = 0.2 or a straight-through notch.

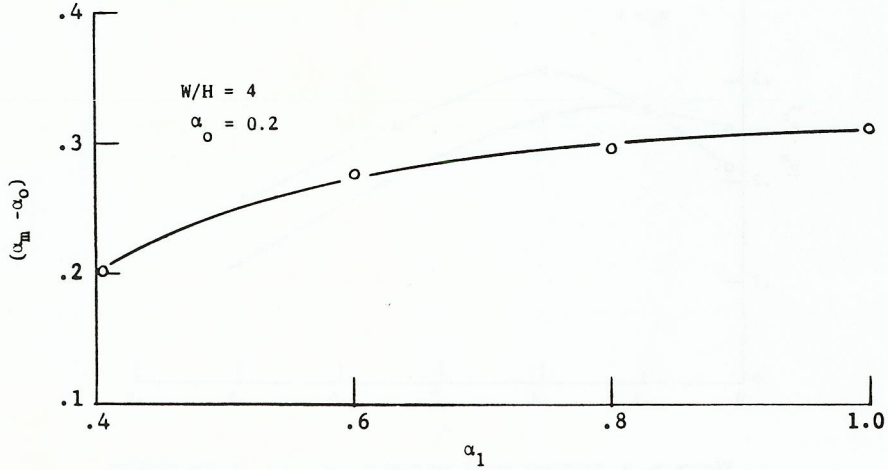

Figure 8. - Relative crack extension $(\alpha_m - \alpha_o)$ at the minimum value of Y* as a function of α_1 for short bar chevron-notch specimens of W/H = 4 and α_o = 0.2.

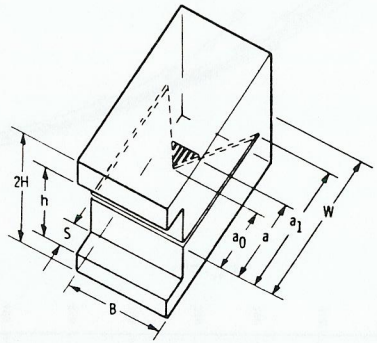

MATERIAL	B	W	H	W/H	h	S	a_0	a_1
Si_3N_4	8.8 - 9.6	15.2	4.5	3.4	6.3	2.5	2.5 - 7.3	7.5 - 15.2
Al_2O_3	25.4	50.8	12.7	4.0	12.7	3.8	10.6 - 22.2	50.8
	25.4	38.1	12.7	3.0	12.7	3.8	8.6 - 17.6	38.1
	12.7	25.4	6.35	4.0	6.3	3.8	4.9 - 11.5	10.2 - 25.4
	12.7	19.1	6.35	3.0	6.3	3.8	1.7 - 6.9	19.1

ALL DIMENSIONS IN mm.

Figure 9.—*Chevron-notch short bar fracture toughness test specimen.*